FAILURE MECHANISM OF COLUMN COMPONENTS AND SYSTEMS OF BRIDGES

Kazuhiko Kawashima[1] and Tomohiro Sasaki[2]

Abstract

This paper outlines a large scale testing program of bridge columns and bridge systems which are planned based on NEES and E-Defense collaboration. Pre-E-Defense study on the premature shear failure mechanism of reinforced concrete columns and the failure mechanism of a bridge system is described. The premature shear failure was the main cause of the bridges which collapsed in 1995 Kobe, Japan earthquake. Cyclic and hybrid loading experiments were conducted to clarify the failure mechanism. Collapsing mechanism of a bridge system which was resulted from progressive failure of bearings and unseating prevention devices was clarified based on the nonlinear dynamic response analysis. Both are planned to be tested using E-Defense.

Introduction

Most extensive damage of bridges in the 1995 Kobe, Japan earthquake was resulted by premature shear failure of reinforced concrete piers with termination of main reinforcements [Kawashima and Unjoh]. Termination of main reinforcements with insufficient development length at several mid-heights as well as overestimated shear strength of concrete and few ties resulted in the extensive damage. Shear strength of concrete was not critical in massive wall piers which were constructed at the early ages. However demand for reducing pier section to mitigate disturbance to river flow in river bridges and using under-space for city streets in urban viaducts resulted in construction of slender piers in which shear strength was critical. However because significant earthquakes did not occur close to bridges in the last three decades, the risk of premature shear failure due to termination of main reinforcements was not recognized until recently.

It was first recognized in 1978 Miyagi-ken-oki earthquake when several bridges suffered damage at their piers. It was again recognized in 1982 Urakawa-oki earthquake when Sizunai Bridge suffered extensive damage at their piers [Asanuma]. The design code was improved in 1980 by reducing the allowable shear stress of concrete and improving the development of main bars [JRA 1980].

Various studies have been conducted for evaluation of the seismic risk and retrofit of the premature shear failure. In 1987 effectiveness of steel jacketing to retrofit of bridge piers was first extensively studied based on a series of unilateral cyclic loading test which was

[1] Professor, Department of Civil Engineering, Tokyo Institute of Technology
[2] Department of Civil Engineering, Tokyo Institute of Technology

conducted jointly by Public Works Research Institute and Metropolitan and Hanshin Expressway Public Corporations [Akimoto et al. and Matsuura et al.]. Aims of the joint research were to develop an evaluation method on the vulnerability of premature shear failure and verify the effectiveness of steel jacket to circular hollow piers and rectangular solid piers. They were studied by the Public Works Research Institute, and Metropolitan and Hanshin Expressway Public Corporations, respectively. As a consequence, steel jacket was implemented to many bridges on Metropolitan and Hanshin Expressways. During the 1995 Kobe earthquake, several retrofitted piers did not suffer damage although un-retrofitted pies which were located very close to the retrofitted piers suffered extensive damage. This shows the effectiveness of seismic retrofit of piers. The evaluation and retrofit methods developed have been used as a standard retrofit of bridge piers with termination of main reinforcements.

Based on a cyclic and hybrid loading test, failure mechanism of several piers which supported a viaduct which collapsed during the 1995 Kobe earthquake was clarified [Ikehata et al.]. Failure modes and levels depending on locations of termination of main bars and shear strength were clarified using 1/7 scaled models.

Because failure mechanism of premature shear failure still has many unsolved problems, and because it was the typical damage in the 1995 Kobe earthquake, a large scale shake table test using E-Defense is planned based on NEES and E-Defense collaboration. A preliminary loading test was conducted at the Tokyo Institute of Technology under the funding of National Institute of Earth Science and Disaster Prevention. This paper briefly introduces the test results.

Specimens and Loadings

Four models as shown in Figure 1 and Table 1 were constructed and loaded. The models have essentially the same property with the models used by Ikehata et al. The model piers are 1.68 m tall and have a circular section with a diameter of 400 mm. This is a 1/7 scaled model of a 11.7 m tall prototype pier with a diameter of 2.8 m. Shear-span ratio is 4.2. Deformed bars with a diameter of 6 mm and 3 mm which were specially made for test was used for longitudinal and tie bars, respectively. The longitudinal reinforcements were set in 3 lines; 36 longitudinal bars for outer and center bars each and 18 longitudinal bars for the inner bars. Thus, 90 longitudinal bars were set in the footing and the column below 220 mm. The number of longitudinal bars was determined so that the longitudinal reinforcement ratio was 2.3 %. The inner and center bars were terminated at 480 mm and 840 mm, respectively, because they were terminated at 3,353 mm and 5,853 mm from the bottom in the prototype pier. Consequently, only outer bars existed above 840 mm from the bottom of the pier. The section between the bottom and 480 mm from the bottom, between 480 mm and 840 mm from the bottom and above 840 mm from the bottom is called hereinafter as sections A, B and C, respectively. Longitudinal reinforcement ratio at sections A, B and C was 0.9 %, 1.8 % and 2.3 %, respectively, as shown in Table 2.

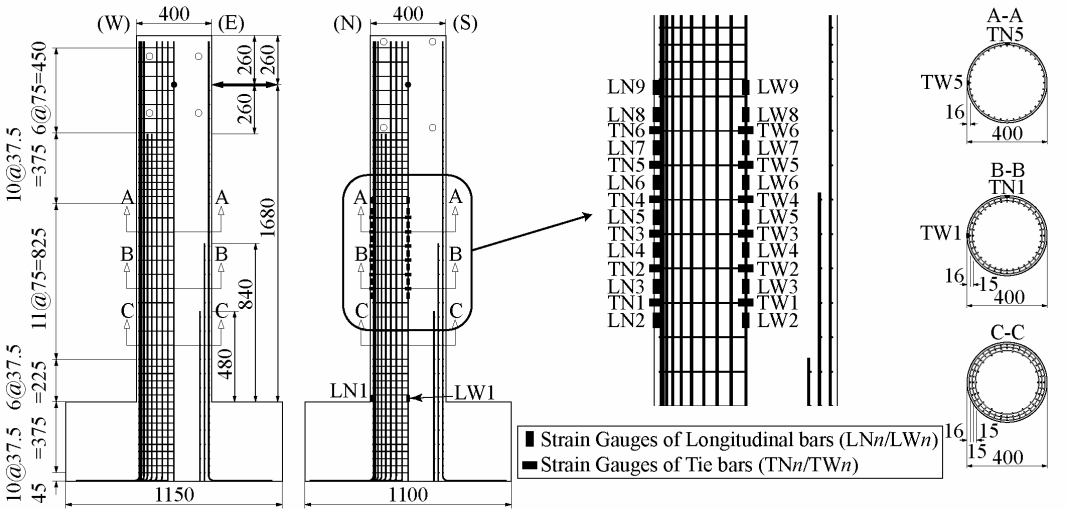

Figure 1 Test Specimens

Table 1 Test Case and Concrete Strength

Test Case	P	C-1	C-2	H
Loading Type	Unilateral Pushover	Unilateral Cyclic	Bilateral Cyclic	Unilateral Hybrid
Concrete Strength	29.6 MPa	26.6 MPa	29.6 MPa	29.8 MPa
Young's modules	25.8 GPa	26.7 GPa	25.8 GPa	36.1 GPa

Table 2 Longitudinal and Tie Reinforcement

Height (mm)	Longitudinal bar		Tie bar	
	Number	Areal Ratio	Interval	Volumetric Ratio
0 - 225	90	0.023	37.5 mm	0.0046
225 - 480	90	0.023	75.0 mm	0.0035
480 - 840	72	0.018	75.0 mm	0.0023
840 - 1050	36	0.009	75.0 mm	0.0011
1050 - 1680	36	0.009	37.5 mm	0.0022

Tie bars were provided to the outer, center and inner longitudinal bars at the section C in the model piers. The volumetric tie reinforcement ratio was assumed as 0.46 % based on the design code [JRA 2002] as shown in Table 2. Therefore spacing of ties was set 37.5 mm. The same spacing was used for outer, center and inner tie bars. The volumetric tie reinforcement ratio was 0.11 % and 0.23 % at sections A and B, respectively. However the tie spacing was reduced to a half at the section below 225 mm from the bottom based on the original design of prototype pier. Amount of tie reinforcement was increased at the top of the pier (above 1,050 mm from the bottom) so that failure did not occur at this section.

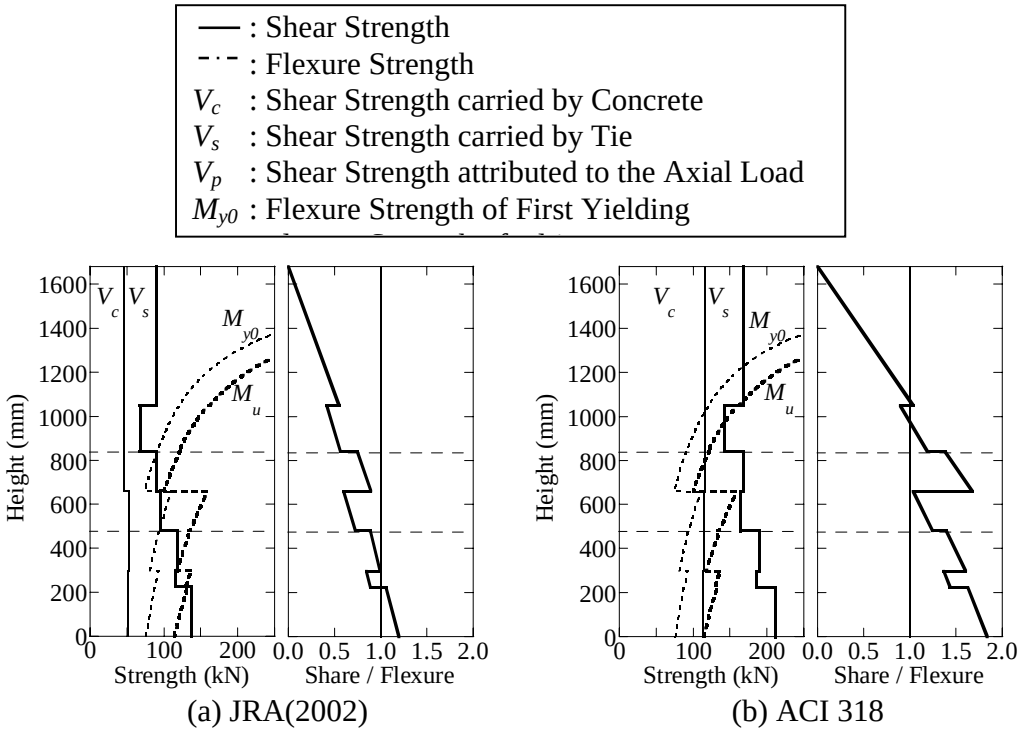

Figure 2 Shear Strength and Flexural Strength of Model Piers

Yield strength, tensile strength and elastic modulus of longitudinal reinforcements were 372.0 MPa, 498.6 MPa and 185.9 GPa, respectively, based on tensile test. Yield strain of longitudinal reinforcements was assumed as 2000 μ in the following analysis. The same properties were assumed for tie bars.

Design concrete strength was 27 MPa. Normal Portland cement was used. Maximum size of aggregates was 13 mm. Concrete strength at the day of the test was in the range of 26.6-29.8 MPa as shown in Table 1.

Figure 2 compares the flexural and shear strengths of the models. Concrete strength of 29.6 MPa is assumed in this estimation. Because shear strength has generally large scattering in its estimation, design equations of JRA and ACI 318 were used. No safety factor was considered in this analysis. It is seen that JRA provide very conservative estimation to the shear strength.

Four loading protocols were used in the test; 1) unilateral pushover loading, 2) unilateral cyclic loading, 3) bilateral cyclic loading and 4) unilateral hybrid loading. Since axial stress of prototype pier was 1.75 MPa, all loadings were conducted under a constant vertical load of 220 kN which corresponded to 1.75 MPa. Lateral drift was used to regulate the loading displacement. Since the first yield and the yield displacement are 9.0 mm and

12.1 mm, respectively, the yield displacement is corresponding to 0.90 % drift.

In the unilateral pushover loading, a pier model was loaded to failure under displacement control. Loading speed was 1 mm/sec until 2.4 % drift. Because the actuator control program had problem, the pier model was loaded by hand with loading velocity of about 0.5 mm/sec over this drift. In the unilateral cyclic loading, loading displacement was step-wisely increased from 0.5 % drift (=8.4 mm) to failure with an increment of 0.5 % drift. The pier was loaded three times at each loading displacement. In the bilateral cyclic loading, a circular orbit was used. The pier was first loaded in the EW direction until the displacement reached 0.5 % drift. From this point, the pier was loaded three times along the circular orbit. Finally, the pier was unloaded to the rest position in the EW direction. This set of loadings was repeated until failure with an increment of 0.5 % drift.

In the bilateral cyclic loading, a circular orbit was used. The pier was first loaded in the EW direction until the displacement reached 0.5 % drift. From this point, the pier was loaded three times along the circular orbit. Finally, the pier was unloaded to the rest position in the EW direction. This set of loadings was repeated until failure with an increment of 0.5 % drift.

In the hybrid loading, the EW component of ground acceleration measured at JR Takatori station during the 1995 Kobe earthquake was used. Intensity of the acceleration was reduced to 15 % (=1/7) of original record assuming that scale factor of mass and acceleration is 1/7. A time-step numerical integration scheme which avoids displacement overshooting using a displacement reduction factor was employed in the simulation system [Shing et al.]. The P-Δ action of actuators was included in the numerical integration of the equations of motion in the hybrid loading test [Nagata et al.]. Damping ratio of 2 % of critical was assumed. The time increment of numerical integration was 0.02 second.

In the above tests, vertical and lateral loading forces, vertical and lateral displacements at the loading points, and strains of longitudinal and tie bars were measured as shown in Figure 1.

Failure Modes and Performance under Unilateral Pushover and Cyclic Loadings

Figure 3 shows the failure mode after the loading and the lateral force vs. lateral displacement hysteresis of the pier under the unilateral pushover loading. Flexural cracks were first developed in tension at the 840 mm from the bottom (refer to Figure 2) where center longitudinal bars were terminated (designated as upper termination zone hereinafter), and they subsequently extended to the bottom of pier in compression. The lateral restoring force took a peak value of 100.8 kN at 1.6 % drift which is hereinafter designated as Point B. Subsequently the lateral restoring force slowly deteriorated to have a sharp deterioration at 3.8 % drift, which is designated hereinafter as Point D.

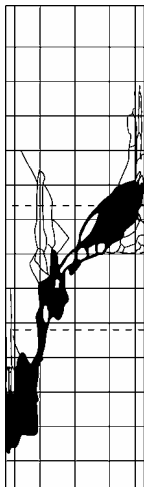

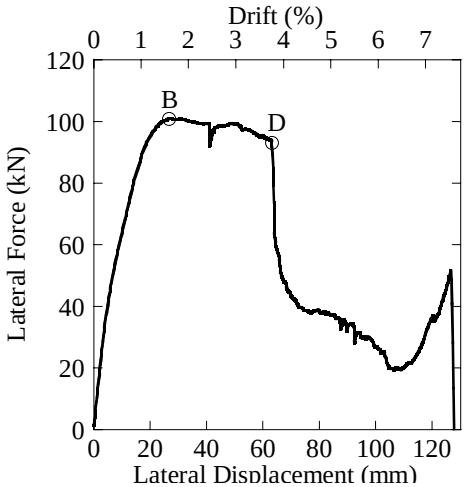

(a) Damage after Loading (b) Lateral Force vs. Lateral Displacement Hysteresis

Figure 3 Unilateral Pushover Loading

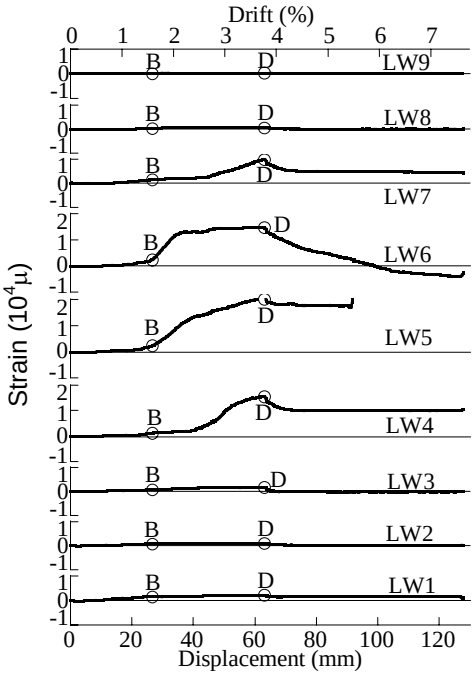

Figure 4 Strains of Longitudinal Bar at W Surface under Unilateral Pushover Loading

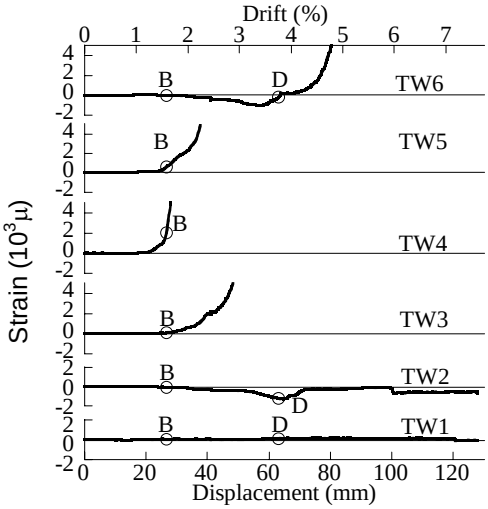

Figure 5 Strains of Tie Bars Parallel to Loading under Unilateral Pushover Loading

Figure 4 shows strains at 9 heights of an outer longitudinal bar which is located middle of the compression and tension fibers (LW1-LW9, refer to Figure 1). It is noted that the longitudinal bar slightly yielded at the plastic hinge (LW1) at Point B, but only limited increase of the strain occurred. Strains of the longitudinal bar at LW4-LW6 (712.5-862.5

mm from the bottom) started to sharply increase at Point B, and they exceeded 10,000 μ at Point D. It should be reminded here that center longitudinal bars were terminated at 840 mm from the bottom of pier (between LW5 and LW6). This resulted in the over 10,000 μ in the outer longitudinal bars at LW4-LW6.

Figure 5 shows strains of ties for outer longitudinal bars parallel to the loading direction (TW1-TW6, refer to Figure 1). It should be reminded here that center longitudinal bars were terminated at the height where TW4 was measured. It is noted that strain at TW4 started to sharply increase slightly before reaching Point B and yielded subsequently. This will be described later. Tie bars at TW5 and TW3 yielded before reaching Point D, however tie bar at TW 6 (975 mm from the bottom) yielded after Point D. This shows that new extension of shear cracks occurred at TW6 after Point D.

On the other hand, Figure 6 shows damage of pier after the unilateral cyclic loading. Flexural cracks were first initiated at the upper termination zone, and they turned into diagonal cracks. They extended subsequently directing to the bottom of pier at 2.0 % drift. But diagonal cracks did not progress furthermore, and separation of the covering concrete and buckling of longitudinal bars progressed at the upper termination zone where flexural cracks were first initiated at 2.5 % drift. Consequently, compression shear failure occurred at the termination zone. The lateral restoring force reached its peak value of 103.4 kN at 1.5 % drift. This lateral force remained until 2.0 % drift with a sudden deterioration at 2.5 % drift.

Figure 7 shows strains of an outer longitudinal bar. Because measurement of bar strains under cyclic loading is extremely difficult, dependable strains have to be carefully evaluated. However it may be seen that longitudinal bars yielded at 0.5 % drift at LW1 (17.25 mm from the bottom of the pier). However strain at LW6 (22.5 mm above the termination of center longitudinal bars) sharply increased to nearly 0.01 (include the exact value) to have the similar value with LW6 at 1.0 % drift, and it further increased over 0.02 at 1.5 % drift. Strain at LW1 did not increase as sharply as LW6. It apparently shows that flexural damage first progressed until 0.5 % drift, however shear failure subsequently occurred after 1.0 % drift.

Figure 8 shows strains of tie bars which are parallel to the loading direction. Strains of tie bars were limited until diagonal cracks occurred at 1.5 % drift. However, over 1.5 % drift tie strain sharply increased at TN4 (same height with termination of center longitudinal bars), which resisted shear after diagonal cracks were initiated.

It is noted that both flexure shear failure and compression shear failure presented above occurred during the 1995 Kobe earthquake. Under unilateral pushover loading, diagonal shear cracks initiated at the upper termination zone extended along the shear cracks. In reality, unilateral pushover loading does not exist during an earthquake. However if a long pulse ground acceleration which is likely included in near-field ground motions is

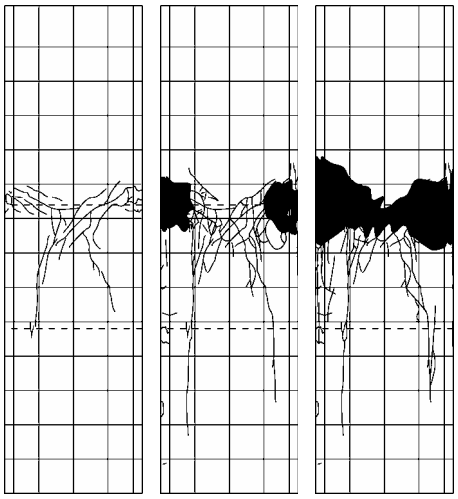

(a) Damage after Loading

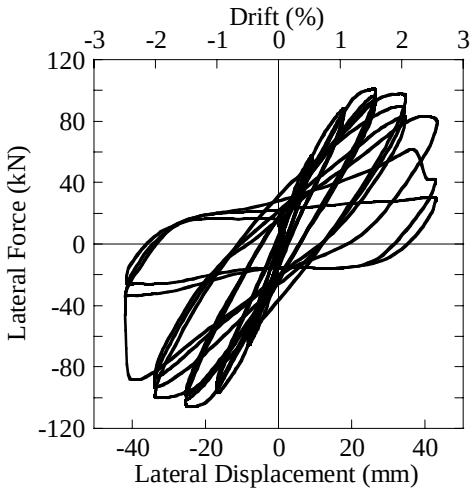

(b) Lateral Force vs. Lateral Displacement

Figure 6 Unilateral Cyclic Loading

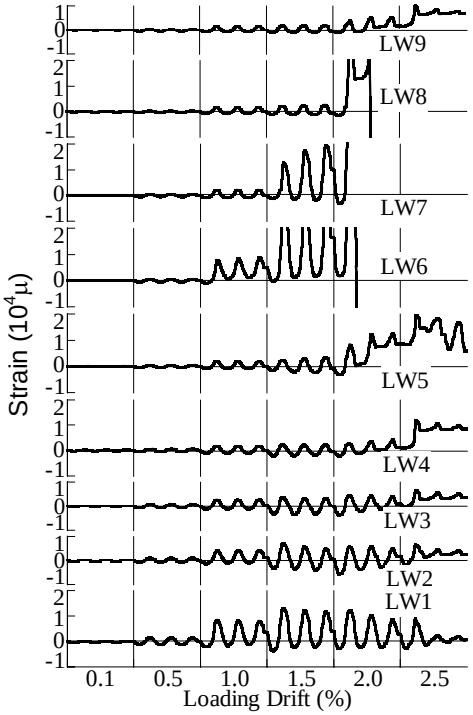

Figure 7 Strains of Longitudinal Bar at W Surface under Unilateral Cyclic Loading

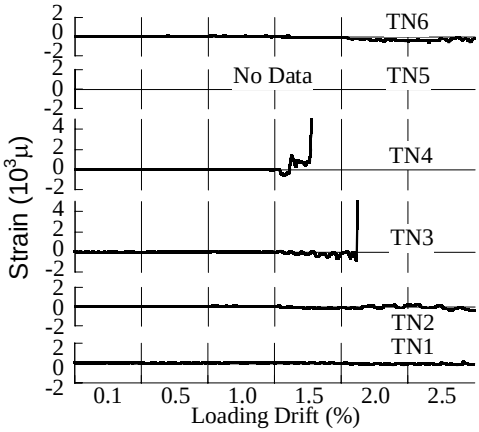

Figure 8 Strains of Longitudinal Bars Parallel to Loading under Unilateral Cyclic Loading

predominant to result in oscillation of a bridge in one direction, the pier may fail in flexure shear. On the other hand, the compression failure is developed at the upper termination under cyclic loading. Because flexural and shear strengths deteriorate at this zone once

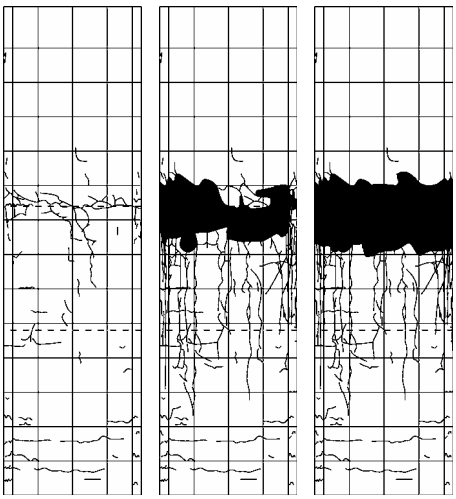

(a) Damage after Loading

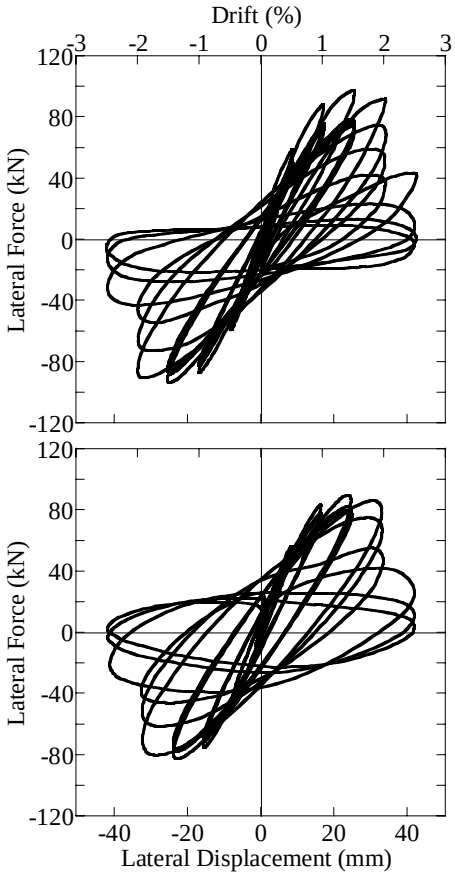

(b) Lateral Force vs. Lateral Displacement

Figure 9 Bilateral Cyclic Loading

compression failure occurs, further extension of diagonal cracks does not occur. Consequently, a pier is likely to fail in compression shear if it is subjected to repeated loading in both directions.

Effect of Bilateral Loading

Figure 9 shows failure after loading and the lateral force vs. lateral displacement hysteresis of the pier under the bilateral cyclic loading. Flexural cracks occurred at the upper termination zone, and the pier failed in compression shear. Failure of core concrete as well as flexural cracks were more extensive under the bilateral loading than the unilateral cyclic loading, however diagonal shear cracks were slightly less under the bilateral loading than the unilateral loading. General trend of the lateral force vs. lateral displacement hystereses are similar to that under the unilateral excitation. However the peak restoring force under the bilateral excitation is nearly 10 % less than that under the unilateral loading.

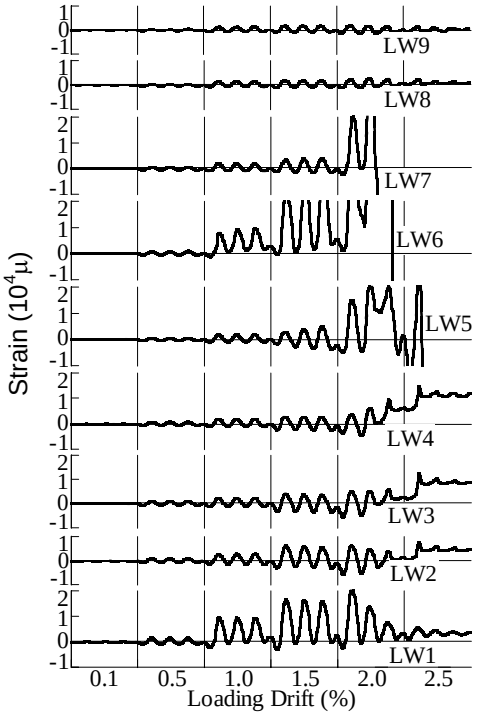

Figure 10 Strains of Longitudinal Bar at W Surface under Bilateral Cyclic Loading

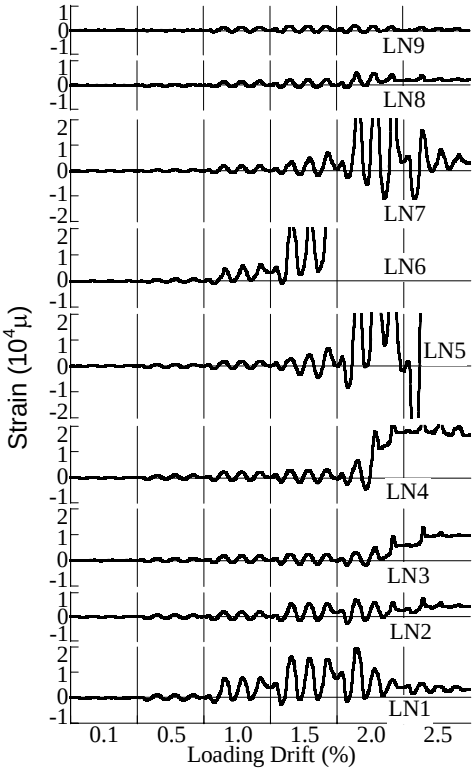

Figure 11 Strains of Longitudinal Bar at N Surface under Bilateral Cyclic Loading

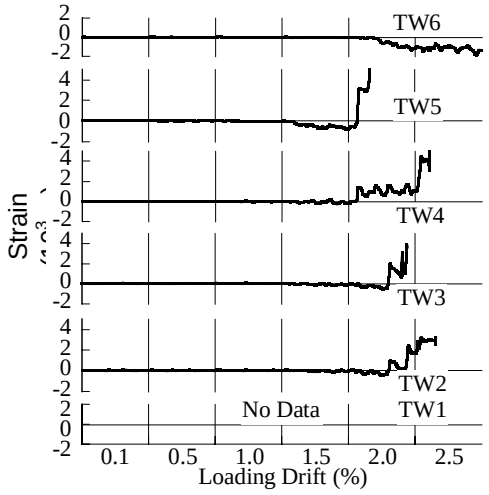

Figure 12 Strains of Tie Bars at W Surface under Bilateral Cyclic Loading

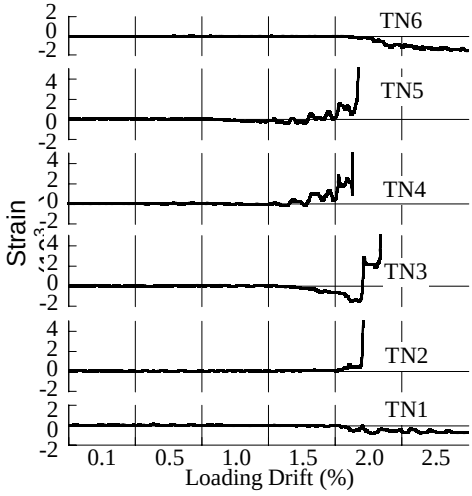

Figure 13 Strains of Tie Bars at N Surface under Bilateral Cyclic Loading

Figures 10 and 11 show strains of longitudinal bars at West and North surfaces. In the longitudinal bars at both surfaces strains at the plastic hinge zone (LW1 and LN1) are dominant than strains at other heights at 0.5 % drift. However, strains at the termination of

inner longitudinal bars (LW6 and LN6) sharply increased to have the similar values with LW1 and LN1 at 1.0 % drift, and they further progressed over LW1 and LN1 at 1.5 % drift.

Figures 12 and 13 show strains of tie bars at N and W surfaces. Strains of tie bars located at the height of termination of inner longitudinal bars (TW4 and TN4) and 75 mm above this height (TW5 and TN5) are larger than strains at other heights. Strains at TW4, TN4, TW5 and TN5 started to increase at 1.5 % drift, and they sharply progressed to nearly yields strain and over 0.02 at 1.5 % drift and 2.0 % drift, respectively.

Performance under Unilateral Hybrid Loading

Figure 14 shows response displacement of the pier as well as the imposed ground acceleration under the unilateral hybrid loading test. Since the pier failed in shear at 4.7 s loading was terminated. The peak displacement at the loading point is 26.0 mm at 1.9 s and -48.9 mm at 2.5 s.

Figure 15 shows failure mode of the column after loading. A large diagonal crack extended from the upper termination of main reinforcements to 300 mm from the bottom. This is very similar to the flexure shear failure which was developed under unilateral pushover loading except several diagonal cracks which were developed in the alternative direction.

Figure 16 shows the lateral force vs. lateral displacement hysteresis of the pier. The peak restoring force at 1.6 % drift is 107.2 kN, which is close to the peak restoring force developed under the pushover loading.

Figure 17 shows strains of longitudinal bars at the W surface located perpendicular to the loading direction. Strain of longitudinal bar at 22.5 mm above the termination (LW6) started to sharply increase at 2.3 s followed by LW7-LW9. Figure 18 shows strains of tie bars. Strains of ties were limited until the pier response first reached 1.5 % drift, but strains at TW4 and TW5 started to sharply increase over this point.

Conclusions

Loading test was conducted to four 1/7 scaled model piers using four loading protocols to clarify the failure mechanism of piers which failed at terminations of main reinforcements with insufficient development length. The following conclusions may be deduced from the results presented herein;

- Failure modes of columns with termination of longitudinal reinforcements with inadequate development length are verey sensitive on loading hysteresis. Flexure shear failure occurred under the unilateral pushover loading, while compression shear failure occurred under the unilateral cyclic loading. Both failure modes occurred during the 1995 Kobe earthquake.

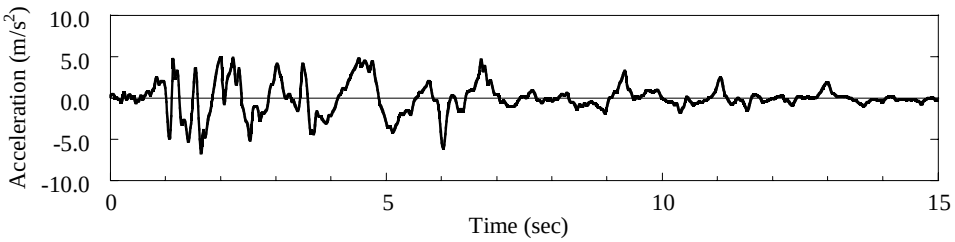

(a) Ground Acceleration

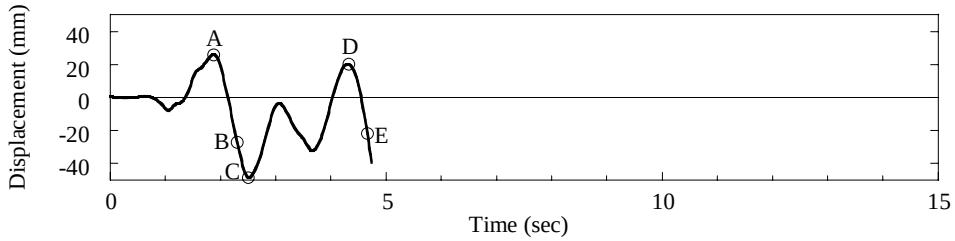

(b) Column Displacement at the Loading

Figure 14 Response of the Model Column under Hybrid Loading

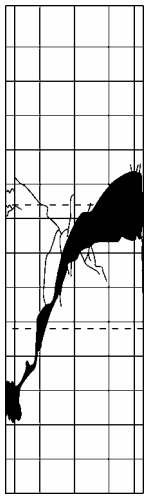

Figure 15 Damage after Loading

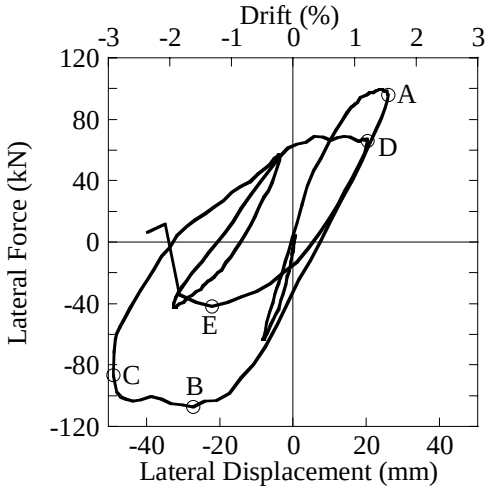

Figure 16 Lateral Force vs. Lateral Displacement Hysteresis

- Flexural shear failure occurred in a coluimn subjected to a near-field ground motion (JR Takatorei record measured during 1995 Kobe earthquake) in unilateral direction. Failure mode is very close to that under the unilateral cyclic loading.
- Flexure cracks occurred more widely and core concrete suffered more significantly under bilateral cyclic loading than unilateral cyclic loading, thus the effect of bilateral loading cannot be ignored.

Acknowledgement

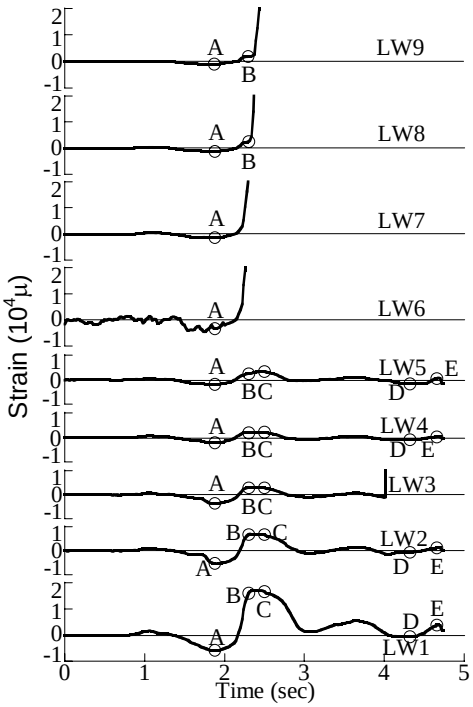

Figure 17 Strains of Longitudinal Bar at W Surface under Unilateral Hybrid Loading

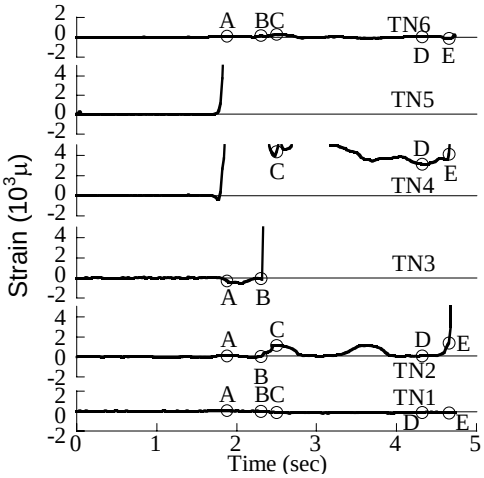

Figure 18 Strains of Tie Bars Parallel to Loading under Unilateral Hybrid Loading

The authors appreciate kind and invaluable guidance of Dr. Ikeda, S., Professor Emeritus, Yokohama National University on the failure mechanism of the prototype bridge and loading method. Great assistance by Messrs. Kijima, K., Paiboon, T., Ogimoto, H., Nagai, T., Wang, Y. and Matsumoto, T. and Mses. Lee, T. Y. and Murotani, N. are greatly acknowledged.

References

ACI Committee 318, "Building Code Requirements for Structural Concrete (ACI 318-95) and Commentary (318R-95)," American Concrete Institute, Farmington Hills, USA, 1995.
Akimoto, T., Nakajima, H., and Kogure, F., "Seismic Strengthening of Reinforced Concrete Piers on Metropolitan Expressway," Proc. First US-Japan Workshop on Seismic Retrofit of Bridges, pp. 258-298, Public Works Research Institute, Tsukuba, Japan, 1990.
Asanuma, H., "Damage of Shauna Bridge," Journal of Civil Engineering, Vol.25, No.11, pp. 15-20, 1983(in Japanese).
Ikehata, S., Adachi, K., Yamaguchi, T., Ikeda, S, "Seismic Performance of RC Bridge Piers based on Quasi-static Dynamic Loading Tests," Proc. JCI, Vol.23, No.3, pp.1255-1260, 2001(in Japanese).
Japan Road Association, "Part V Seismic Design-Design specifications of Highway Bridges," Maruzen, Tokyo, Japan, 1980, 1990, 1996, 2002.

Kawashima, K. and Unjoh, S., “The Damage of Highway Bridges in the 1995 Hyogo-ken Nanbu Earthquake and Its Impact on Japanese Seismic Design,” Journal of Earthquake Engineering, Vol. 1, No. 3, pp. 505-541, 1997.
Kowalsky, M. J., Priestly, M. J. N., “Improved Analytical Model for Shear Strength of Circular Reinforced Concrete Columns in Seismic Regions,” ACI Structural Journal, Vol.97, No.3, 2000.
Matsuura, Y., Nakamura, I. and Sekimoto, H., “Seismic Strengthening for Reinforced Concrete Bridge Piers of Hanshin Expressway,” Proc. First US-Japan Workshop on Seismic Retrofit of Bridges, pp. 299-317, Public Works Research Institute, Tsukuba, Japan, 1990.
Nagata, S., Kawashima, K. and Watanabe, G., “Effect of P-Δ Action of Actuators in a Hybrid Loading Test,” Proc. 13th World Conference on Earthquake Engineering, Paper No. 881, Vancouver, Canada, 2004.
Priestley, N.M.J., Seible, F. and Calvi, M., “Seismic Design and Retrofit of Bridges,” John Wiley & Sons, New York, USA, 1996.
Shing, P, B., Vannan, M.T. and Cater, E., “Implicit Time Integration for Pseudodynamic Tests,” Earthquake Engineering and Structural Dynamics, Vol. 20, pp. 551-576, 1991.